Operational Calibration of the Imagers and Sounders on the GOES-8 and -9 Satellites

Michael Weinreb, Michael Jamieson, Nancy Fulton, Yen Chen, Joy Xie Johnson, James Bremer, Carl Smith, and Jeanette Baucom

ABSTRACT

The operational in-orbit calibration of the GOES-8 and -9 imagers and sounders is described. In the infrared channels, the calibration is based on observations of space and an on-board blackbody. The calibration equation expresses radiance as a quadratic in instrument output. To suppress noise in the blackbody sequences, the calibration slopes are filtered. The calibration equation also accounts for an unwanted variation of the reflectances of the instruments' scan mirrors with east-west scan position, which was not discovered until the instruments were in orbit. The visible channels are not calibrated, but the observations are provided relative to the level of space and are normalized to minimize east-west striping in the images. Users receive scaled radiances in a GVAR (GOES VARiable format) data stream. The procedure users may apply to transform GVAR counts to radiances, temperatures, and "mode-A" counts is described.

1. INTRODUCTION

The National Oceanic and Atmospheric Administration (NOAA) operates a system of Geostationary Operational Environmental Satellites (GOES) to provide frequent visible and infrared images of the Earth as well as quantitative meteorological data products, such as estimates of atmospheric temperature and moisture profiles, winds, and precipitation. The imagery is well-known to the general public through televised weather reports. The GOES-8 and -9 satellites, launched on April 13, 1994, and May 23, 1995, respectively, are currently stationed at 36,000 km above the equator at 75W and 135W longitudes, respectively. Both carry an Earth-atmosphere imager and an atmospheric sounder[1-3]. These instruments observe the Earth in a total of 24 spectral intervals ("channels") at wavelengths between 0.6 μm and 14.7 μm. The imager makes observations in five channels (Table 1), which are isolated by stationary filters in its optical chain. Each channel utilizes a separate linear north-south array of detectors--eight detectors in channel 1, two in channels 2, 4, and 5, and one in channel 3. The sounders observe in 19 spectral intervals (Table 2).

Table 1. Characteristics of imager channels

Channel	Nominal center wavenumber (cm^{-1})	# of detectors in N-S array	Detector FOV (km)	Detector material
1	16000 (visible)	8	1	Si
2	2555	2	4	InSb
3	1480	1	8	HgCdTe
4	935	2	4	HgCdTe
5	835	2	4	HgCdTe

Table 2. Characteristics of imager channels

Channel	Nominal center wavenumber (cm^{-1})	Detector material	Channel	Nominal center wavenumber (cm^{-1})	Detector material
1	680	HgCdTe	10	1345	HgCdTe
2	696	HgCdTe	11	1425	HgCdTe
3	711	HgCdTe	12	1535	HgCdTe

4	733	HgCdTe	13	2188	InSb
5	748	HgCdTe	14	2210	InSb
6	790	HgCdTe	15	2245	InSb
7	832	HgCdTe	16	2420	InSb
8	907	HgCdTe	17	2513	InSb
9	1030	HgCdTe	18	2671	InSb
			19	14367(visible)	Si

The spectral intervals in the infrared are isolated by a rotating wheel of filters. The filters are placed on the wheel in three concentric circles, which correspond to the channels of the three wavenumber regions--longwave (channels 1-7), midwave (channels 8-12), and shortwave (channels 13-18). Adichroic beamsplitter and a fixed filter isolate the visible channel. There is a north-south array of four detectors for each of the three infrared wavenumber regions, and a similar four-detector array for the visible. Each detector has a field of view (FOV) of approximately 8 km. Imager outputs are transmitted to the ground station as 10-bit words, sounder outputs as 13-bit words.

Before the launch of each satellite, the radiometric performance of the instruments was characterized in an extensive program of pre-launch tests conducted by their manufacturer (ITT, Ft. Wayne, IN) and by the GOES I-M prime contractor (Space Systems/Loral, Palo Alto, CA). The form of the in-orbit infrared calibration equation and some of the coefficients were determined from these tests. Despite the extensive testing before launch, the data from orbit revealed unforeseen performance anomalies, most notably a variation in the emissivity of the instruments' scan mirrors with east-west scan position that necessitated a change in the in-orbit calibration equation and procedures. Operational processing by the new calibration equation was initiated months after the launches of the GOES-8 and GOES-9 satellites and at different times for different instruments.

The purpose of this memorandum is to document the complete calibration processing, including the post-launch modification for the scan-mirror emissivity variation, which NOAA carries out in its ground-system computers. This is covered in sections 3-6, which follow a short description of the calibration data in section 2. Section 7 describes the digital data that users receive, which, in infrared channels, are scaled radiances, and, in visible channels, normalized instrument output relative to the level of space. Appendix A presents the procedure for users to transform the scaled radiances to physical radiances and brightness temperatures.

2. INFRARED CALIBRATION DATA

In orbit, the imagers and sounders periodically view space and their on-board warm blackbodies to acquire data for calibrating their infrared channels. Each instrument's blackbody is in front of its entire optical chain and fills its optical aperture. (This is in contrast to the Visible Infrared Spin-Scan Radiometer [VISSR] and VISSR Atmospheric Sounder [VAS] instruments, carried on earlier geostationary satellites. In those instruments, the calibration target was behind the fore-optics, necessitating modelling of the radiative contribution of the fore-optics in the calibration[4].) The data acquired at the blackbody looks (and associated space looks) are used for inferring the instruments' calibration slopes (radiance increment per output count), which are the reciprocals of the responsivities. The data from the space looks allow us to infer the calibration intercepts (radiance at zero counts).

To preserve the precision of the measurements, the instruments are calibrated often, because temperatures on a three-axis stabilized satellite such as GOES vary diurnally by tens of degrees Kelvin. The diurnal variation of the intercepts, which measure the intensity of the radiation emitted by the instrument itself, is considerably greater than that of the slopes, which depend weakly on such quantities as the background flux on the detectors and the temperature of the electronics. Therefore, space looks are executed more frequently than blackbody looks. For the imagers, another reason to view space as frequently as possible is provided by the presence of 1/f noise[5] in the channels that use photoconductive HgCdTe detectors. The 1/f noise manifests itself as a drift in the imager's output in the time between the space clamps. While viewing space, the imagers execute their DC signal restores ("space clamps"), which reset the zero-radiance output to a predetermined value (nominally 970 counts). The more frequent the clamps, then, the less severe the drifts. The sounders chop the signal from the scene at a frequency of approximately 50Hz against opaque "teeth" located between the filters on the filter wheels, which largely suppresses the effects of 1/f noise.

The intervals between calibration measurements are listed in Table 3. For the imager, the space looks for calibration all involve space clamps. Currently, the 2.2-sec space-look interval is used for imaging the full Earth, and the 36.6-sec interval for imaging smaller sectors. The 9.2-sec interval is not used for routine imaging. This selection of intervals represents a compromise between radiometric precision and scheduling requirements imposed by the NOAA/National Weather Service.

Table 3. Intervals between calibration measurements

Measurement Type	Imager	Sounder
Space	2.2, 9.2, or 36.6 sec	2 min

Blackbody	30 min	20 min

For the sounder, a space look may interrupt a scan line in progress. A space look consists of the acquisition of 40 samples of data at a location at least 0.5 degrees away from the Earth. Typically, this requires a total of approximately 8 sec, of which 4 sec is devoted to taking the data and the rest to slewing and settling of the scan mirror. A blackbody sequence, which may interrupt a frame (a pre-defined rectangular target area on the Earth) in progress, consists of acquisition of 40 samples from a view of space (4 sec), data for a check of the linearity of the electronics (1.6 sec), and 40 samples during the view of the blackbody (4 sec). The entire sequence requires approximately 55 sec, of which approximately 45 sec are devoted to slewing and settling of the scan mirror. The view of the blackbody occurs approximately 23 sec after the view of space.

For the imager, space looks occur only during scan reversals, i.e., when the direction of the scan mirror's motion reverses between two scans in opposite directions. The location is at least 0.5 degrees from the edge of the Earth. The sequence of events at the reversal is acquisition of approximately 400 samples from a view of space, the DC restore (clamp), and another acquisition of 400 samples of data from a view of space immediately following the clamp. These two views of space are called the "pre-clamp" and "post-clamp" views, respectively. Acquisition of 400 samples requires approximately 73 msec, and an entire scan reversal, including the clamp and the two space views requires 200 msec. The purpose of acquiring two sets of data at each space look is to combat the effect of drifts during the period of data-taking on the Earth that occurs between any two space looks. The calibration intercepts are interpolated (see below) in time from the post-clamp of the first space look to the pre-clamp of the second.

Imager blackbody sequences occur every half hour between frames. A sequence consists of acquisition of 400 samples from the post-clamp phase of a space look (73 msec), 1000 samples during the view of the blackbody (183 msec), and 400 samples (73 msec) from the pre-clamp phase of the space look following the blackbody. The entire sequence requires approximately 44 sec, and almost all of that is dedicated to the slewing and settling of the scan mirror. The blackbody observations take place approximately 18 seconds after the first space look and 18 seconds before the second. To minimize the effect of drifts that will almost certainly affect the instrument outputs in the intervals between the views of the blackbody and space, we interpolate the outputs from the two space looks to the time of the blackbody look. This accounts for the linear component of the drifts but does nothing to correct for higher-order components[5].

3. INFRARED CALIBRATION EQUATIONS AT LAUNCH

The calibration equation relates the radiance R from the scene to the output X of the instrument, which is in ten-bit counts for the imager and 13-bit counts for the sounder. There is a specific calibration equation for each detector of each channel. The calibration equation that was in use at the time of the launches of both GOES-8 and GOES-9 (but was modified several months later, as will be described below) is

Equation 1

$$R = qX^2 + mX + b.$$

where q, m, and b are the coefficients and will be described below. The equation is quadratic to allow for possible non-linearities in sensor response, which affect primarily the longwave and midwave channels. For a particular channel and detector, the radiance R is the average of the spectral (monochromatic) radiance over the spectral response function for that channel and detector, i.e.,

Equation 2

$$R = \frac{\int R(\nu)\,\Phi(\nu)\,d\nu}{\int \Phi(\nu)\,d\nu},$$

in which n is the wavenumber (in cm^{-1}), F the spectral response function, and R(n) the spectral radiance. The integrals are carried out over the range of n for which F is non-zero. Units of R are $mW/(m^2\text{-}sr\text{-}cm^{-1})$.

The value of q, the coefficient of the quadratic term, was (and is) known a *priori*, having been determined from measurements made by ITT before launch[6]. Values of q were determined in each channel as a function of instrument operating temperature and detector temperature. The statistical precision of each measurement of q was usually between 5 and 10%. Provision was made in the in-orbit processing to allow q to depend on the actual instrument and detector temperatures. However, analyses of the pre-launch data indicated that, in most cases, q seemed to vary randomly with instrument temperature and to be only weakly correlated with detector temperature[7]. As a result, for in-orbit calibrations we use a single value of q in each channel. It is the unweighted mean over all instrument and detector temperatures.

The coefficients m and b, termed the slope and intercept, respectively, are determined during in-orbit operations as follows: From the data in each blackbody sequence, m is given by

Equation 3

$$m = [R_{bb} - q(X_{bb}^2 - X_{sp}^2)]/(X_{bb} - X_{sp}),$$

where subscripts bb and sp refer to data taken from views of the blackbody and space, respectively. The radiance R_{bb} of the blackbody is computed from its temperature, which, for both the sounder and the imager, is indicated by eight thermistors. In the computations, we average nine samples from each thermistor and average over the eight thermistors. For efficiency in the real-time computation, the radiance values are computed not by Eq. (2) but from cubic polynomials in temperature T,

Equation 4

$$R = \sum_{i=0}^{3} a_i T^i .$$

The coefficients a_i were derived before launch[6] from a fit of a cubic to a table of temperatures vs blackbody radiances at every 0.1K between 270K and 310K. This range includes every temperature the blackbodies are expected to assume in normal operations in orbit. The blackbody radiances were computed with Eq. (2) in which R(n) is the Planck function B(n,T), given by

$$B(\nu,T) = \frac{c_1 \nu^3}{\exp(c_2 \nu/T) - 1},$$

where the coefficients c_1 and c_2 are the two radiation constants, given by

$c_1 = 1.191066 \times 10^{-5}$ mW/(m^2-sr-cm^{-4});

$c_2 = 1.438833$ K/cm^{-1}.

The errors of the polynomial approximation are at least an order of magnitude less than the expected noise in each channel

The values of X_{sp} and X_{bb} require elaboration. For the sounder, X_{sp} is the average of the 40 samples at the space look preceding the blackbody look. For the imager, X_{sp} is determined from the 400-sample averages for the space looks preceding and following the blackbody look. The value at the time of the blackbody look is estimated by interpolation on time between the two space looks. The interpolation

reduces the effect of drifts over the period of the blackbody sequence[5]. The values of X_{bb} are the averages of the 40 samples (sounder) or 1000 samples (imager) acquired during the blackbody view.

From data collected at each space look, b is determined from

Equation 5

$$b = -m X_{sp} - q X_{sp}^2 .$$

The value of X_{sp} is the average of the 40 samples (sounder) or 400 samples (imager) acquired at the space view. For the imager, the intercepts are computed and saved for both the pre- and post-clamp views. As space looks occur more frequently than the blackbody looks, intercepts are updated more often than are the slopes.

For each pixel, the radiances were computed from Eq. (1) with the values of m and b from Eqs. (3) and (5). For the imager, to remove the effects of drift between the space looks, we update the value of b at each pixel by interpolating between the post-clamp view at the preceding space look and the pre-clamp view at the following space look, as was described previously.

4. REVISION FOR VARIATION IN SCAN-MIRROR EMISSIVITY

Shortly after the GOES-8 instruments began operating in orbit, it was observed that the outputs of the imager and sounder channels at wavelengths between 6 and 14 μm varied with the east-west position of the field of view. This was most apparent when the instruments viewed space. As an example, Fig. 1 shows raw imager data from east-west scans of space above the north pole at three different times of day. Although the scans extend approximately 19° in the east-west direction (which slightly exceeds the 17.4° width of the Earth), they correspond to a mechanical scan-mirror rotation of half that, or 9.5°. (In Fig. 1, the abscissa is mechanical scan mirror angle.) At a scan-mirror angle of 45°, the imager views the meridian directly below the satellite; at angles of 40° and 50°, the imager views space beyond the west and east sides of the Earth, respectively. The differences in output between the east and west sides of the scans correspond to an artificial temperature difference of approximately 150K. More to the point, there were also radiometric errors--as large as several degrees Kelvin in brightness temperature--in observations of the Earth, although they were masked by the variability in the scene. Similar angle dependences and radiometric errors were also observed later in data from the GOES-9 instruments. The cause of this behavior is believed to be an absorption feature of the silicon oxide coatings of the scan mirrors, which causes the mirrors' emissivities to vary with the incidence angle of the incoming radiation. Processing changes[8] (described below) to eliminate these radiometric errors were made operational in

April 1995 and August 1995 for the GOES-8 and GOES-9 imagers, respectively. For the GOES-8 and GOES-9 sounders, the corrections became operational in June and April 1996, respectively.

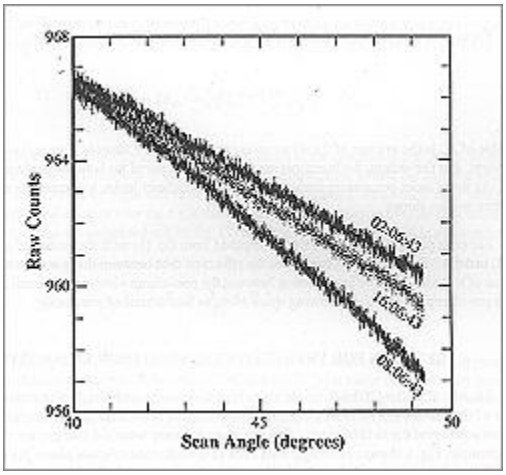

Fig. 1. Raw output (counts) of channel 5 (12 μm)

of GOES-9 Imager from east-west scan of space.

The data are labeled by the time of day in GMT. The abscissa is mechanical scan angle. Since the imager was constructed so that increasing counts correspond to decreasing brightness temperature, this figure makes it appear as if the temperature of space were increasing from west to east.

4.1 Generalized infrared calibration equations

The processing change invokes a generalization of the calibration equation to include the emission and reflection of the scan mirror. The generalized calibration equation is

Equation 6

$$(1 - \epsilon[\theta])\, R + \epsilon[\theta]\, R_M = qX^2 + mX + b,$$

where R, X, q, m, and b are defined as in Eq. (1). The quantity e is the emissivity of the scan mirror, and it is a function of scan angle q. The procedure for determining e[q] is described in the next section. The parameter R_M is the radiance of the scan mirror. This radiance is computed via Eq. (4) from the

temperature of the scan mirror, which is monitored by a thermistor embedded in its structure. The validity of Eq. (6) depends on the relationship[9]

$$\rho = 1 - \epsilon,$$

in which r is the reflectance and e the emissivity in a particular direction of an opaque, specularly-reflecting surface.

Equation (6) differs from Eq. (1) on the left hand side, where now the scene radiance R is multiplied by (1 - e) instead of 1; this represents the reduction in the radiation received from the scene as the reflectance of the scan mirror is reduced from 1 to 1 - e. Also, there is a second term, which represents the radiation emitted by the scan mirror.

In orbit, the processing goes as follows: At each blackbody look, m is determined from

Equation 7

$$m = [r_{bb} - q\,(X_{bb}^2 - X_{sp}^2)]/(X_{bb} - X_{sp}),$$

where the variables are defined as in Eq. (3). However, r_{bb} is not simply the radiance of the blackbody R_{bb}, but is related to it by

Equation 8

$$r_{bb} = (1 - \epsilon[45])\,R_{bb} + (\epsilon[45] - \epsilon[sp])R_{M,bb},$$

where $R_{M,bb}$ is the radiance of the scan mirror computed from its temperature at the time of the blackbody sequence. The quantity e[45] is the scan mirror's emissivity when it is at the blackbody position, for which the angle of incidence of the incoming radiation is 45°. Similarly, e [sp] is the emissivity at the space look position, which will have an incidence angle of either 40° or 50°, depending upon which side of the Earth the space look occurs. (For the imager, 40° is on the west, while for the sounder it is on the east.)

From Eqs. (7) and (8), it would appear that m depends on the side of Earth on which the space view occurs. Nevertheless, it is, in fact, a property only of the instrument--it is essentially the reciprocal of the responsivity of the radiometer downstream of the scan mirror--and it does not depend on space-view side.

At each space look, b is determined from the equation

$$b = -m X_{sp} - q X_{sp}^2 + \epsilon(sp) R_{M,sp},$$

where $R_{M,sp}$ is the mirror radiance at the time of the space look. The value of b may depend on space-clamp side.

It is convenient to define the quantity b_e, as

Equation 9

$$b_e = -m X_{sp} - q X_{sp}^2.$$

Then, for each pixel, the radiances are computed from

$$R = \{qX^2 + mX + b_e - (\epsilon[\theta] - \epsilon[sp])R_{M,sp}\}/(1 - \epsilon[\theta]),$$

where m is from Eq. (7), and e(q) is e evaluated at the scan angle (pixel position) q.

For the imager, the interpolation of space-look counts within the blackbody sequences, and the interpolation of the intercepts between space looks, are still carried out, as described previously.

4.2 Derivation of emissivities

The scan-mirror emissivity values were determined soon after launch from in-orbit observations of space between the extreme west and the extreme east. Data for a number of scans were averaged to reduce random noise. For the sounders, the instrument output varies not only with scan position, but with time, as the temperature of the instrument changes over the minute or so required for each scan. (This is not a problem for the imagers, which clamp on space every few seconds.) We removed the temperature-driven drifts from the sounder data after estimating them by regression on the optics temperatures.

Emissivities were derived separately for each detector in each channel of each instrument. In the following, we suppress reference to instrument, channel, and detector, since the procedure was the same for all of them. Since measurements on space were available at all values of q, not just at the east and west limits, the definition of the calibration slope in Eqs. (7) and (8) could be simplified to

$$m = \{[1 - \epsilon(45)]R_{bb} - q[X_{bb}^2 - X_{sp}^2(45)]\}/\{X_{bb} - X_{sp}(45)\},$$

where $X_{sp}(45)$ is the instrument output in counts when it views space at a scan angle of 45°. The emissivity was given by

$$\epsilon(\theta) = \epsilon(45) + \{m[X_{sp}(\theta) - X_{sp}(45)] + q[X_{sp}^2(\theta) - X_{sp}^2(45)]\}/R_M ,$$

where R_M is the radiance of the mirror computed from its temperature during the scans, and $X_{sp}(q)$ is the instrument's output in counts when it views space at scan angle q. The emissivities at 45° in all imager and sounder channels were provided from laboratory measurements on witness samples[10].

The entire process was carried out for data collected approximately once an hour for 24 hours. A daily-average profile of e vs q was then computed as the average over all hours.

For each channel, we fitted a quadratic, i.e.,

$$\epsilon(\theta) = a_0 + a_1\theta + a_2\theta^2 ,$$

to the profiles of emissivity vs q. (Also, the variable q was transformed to become the east-west position of the scan mirror expressed in inductosyn increment numbers, which is uniquely related to scan angle.) This produced the coefficients a_0, a_1, and a_2. They are stored in a database in the ground-system computer and are used in the processing to generate the emissivities vs angle.

Approximately once every three months, new emissivity-vs-angle profiles are computed from east-west scans of space, as previously described. Thus far, the profiles have changed slightly for some instruments, and not at all for others, since the launches of the GOES-8 and -9 satellites.

Figure 2 attests to the success of the generalized calibration equations. It shows the radiances of space vs scan angle derived from the original calibration equations ("before") and the generalized equations ("after") in channels 4 (10.7 μm) and 5 (12 μm) of the GOES-8 imager. The generalized equations removed apparent east-west radiance differences of approximately 1mW/(m^2-sr-cm^{-1}) and 2 mW/(m^2-sr-cm^{-1}) in channels 4 and 5, respectively.

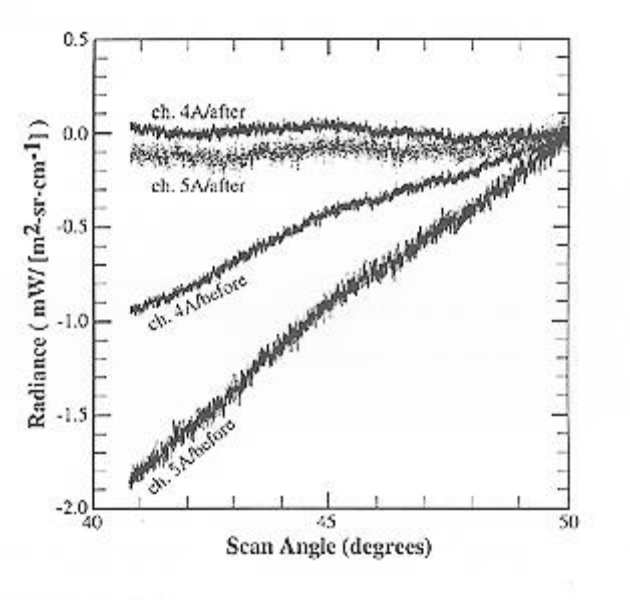

Fig. 2. Radiances of space vs mechanical scan angle (degrees)

in channels 4 and 5 of GOES-8 Imager.

The label, "before", indicates data before correction for scan-mirror emissivity variation; "after" indicates data after correction. The uncorrected radiance values are negative because the calibration establishes the zero-radiance level at the space clamp, which in this case was on the east.

5. NOISE SUPPRESSION IN IMAGER BLACKBODY CALIBRATIONS

Although the effects of drift and 1/f noise in the Imagers' blackbody sequences are reduced by the interpolation of the space-count value to the time of the blackbody view, a significant amount of random variation (henceforth termed "noise") occurs in the time series of computed calibration slopes. The asterisks in Figure 3 delineate the time series of slopes, computed every 30 min, from the two detectors in channel 4 of the GOES-8 imager. Apart from noise, these plots exhibit diurnal variation in the slopes with peak-to-peak amplitude of approximately 2%. This is a true variation in instrument responsivity, caused primarily by variations in the background radiation on the detectors. This is expected, causes no errors, and will not be discussed further. However, the noise is a problem. It induces errors in the radiances, and it also introduces systematic striping[11] in the images, which is often noticeable. The reader is reminded that each of the two detectors in this channel generates alternate lines of each image. The slope error for either detector induces a systematic error in the radiance at every scene (pixel) observed by that detector for the 30 min following the calibration. Since these errors are, to a large extent, uncorrelated between the two detectors, the systematic errors in the radiances will usually be different for the two detectors, and the image will appear striped. The characteristics of the striping will change every 30 minutes, as the errors

vary from one blackbody sequence to the next. The magnitude of the striping in images from channel 4 of the GOES-8 imager is typically of the order of 0.1K and 0.4K for scenes at 300K and 200K, respectively.

The calibration processing in the ground system applies an averaging technique to smooth out the slope noise. It would not be desirable to average over a significant fraction of a day, since that would introduce errors by removing true diurnal variation. Instead, a two-hour running window is used. To achieve enough smoothing, we include the slopes in the same two-hour interval from each of the previous nine days. It is expected that the diurnal pattern of the slopes would not change significantly over nine days. Data from more than nine days previous are not included, because seasonal changes in the diurnal pattern may become significant over such a long period and skew the average. The averaging includes the data from the current time--for which the current slope and the slopes from the previous hour are available; the data from the previous eight days--for which slopes from five blackbody sequences in the full two-hour window centered on the current time are available; and, finally, the data for the ninth day before the current day--for which the slopes for the current time and one hour afterwards are available. In the averaging, the slopes are weighted inversely according to their displacement in time, both in days and in minutes within the two-hour window, from the current blackbody sequence. Averaged slopes, plotted in Fig. 3 as the solid lines, reduce the scatter exhibited by the original slopes. The averaging also reduces the frame-to-frame variation in striping[11].

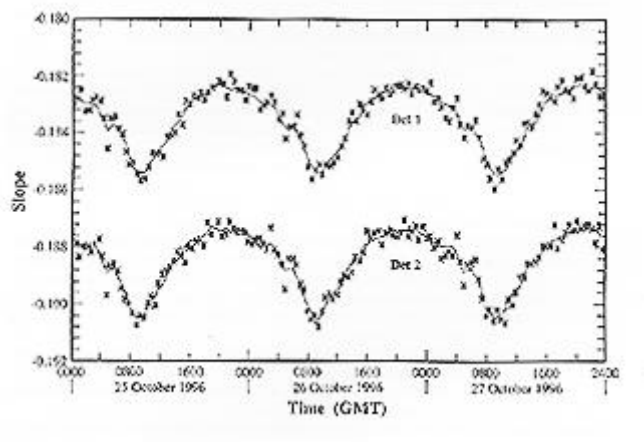

Fig. 3. Time series of calibration slopes for detectors 1 and 2 of channel 4 of the GOES-8 Imager. Units of slopes are [mW/(m^2-sr-cm^{-1})]/count.

Asterisks are unaveraged; solid lines, averaged.

6. PROCESSING OF VISIBLE-CHANNEL DATA

The imager uses a north-south array of eight silicon diode detectors to image the earth, and the sounder uses an array of four similar detectors, primarily for cloud detection. With each east-west or west-east

traversal of the scan mirror, the imager thus produces eight adjacent east-west lines and the sounder, four. These detectors are not calibrated on orbit, but their data are processed to maintain image quality, as is described in the remainder of this section.

6.1 Normalization (destriping)

Without in-orbit calibration, the uncompensated responsivity differences among the elements of the visible-channel detector array can result in the appearance of artificial east-west stripes in the images. This striping can be reduced by the normalization of each detector's output to the output of a stable reference detector. The normalization is applied in real time at the Command and Data Acquisition (CDA) station at Wallops, VA, through application of normalization look-up tables (NLUTs) to the raw scene data.

The technique for generating NLUTs is carried out off-line and involves matching the empirical distribution functions (EDFs) of the raw data from each detector to that of the reference detector.12 The reference detectors, listed in Table 5 (for the imagers only), were chosen from considerations of long-term stability and maximal usage of the count range of the data system without clipping at the upper and lower limits.

Image striping is monitored daily at NOAA. Striping in images from the GOES-8 imager has been minimal, even in the absence of normalization. Since March 29, 1995, the data have been normalized to remove a small amount of striping, but the detectors have been so stable that there had been no need to update the NLUT until May 1996, when relativization (see below), was introduced. At that time a new NLUT was made operational, and it is expected that it will remain valid for many months. A similar statement can be made for the visible channel of the GOES-9 imager. The first NLUT became operational on July 31, 1995, and it remained valid until April 1996, when relativization was introduced, whereupon a new NLUT was implemented.

Visible data from the sounders are not being normalized as of this writing. For the GOES-8 sounder, normalization had been applied in the period between March 29, 1995, and June 19, 1996. On June 19, 1996, when relativization was introduced, it was found that normalization was not needed, and it was discontinued. Visible data from the GOES-9 sounder were never normalized.

6.2 Relativization

The signal from any scene is the instrument's output while viewing the scene, minus its output when viewing space. Until the spring of 1996, however, the data in the visible channels of the GOES-8 and GOES-9 sensors were transmitted to users in absolute counts, i.e., scene counts without the space

counts subtracted out. In this form, the data were consistent with the visible-channel data from other NOAA satellites past and present.

The process of differencing the signals from the scene and space is termed "relativization," because its outcome is a signal relative to space. Relativization removes effects of the zero-signal background, long-term drifts, and detector-to-detector offset differences. For the imagers, relativizing the signals is usually not important under normal conditions. The outputs of the photodiode detectors are relatively stable in time and consistent among detectors. The space clamps continually set the count level from space at approximately 29 counts, thereby preventing significant drifts caused by temperature changes. And there are no detectable drifts from 1/f noise in the visible channels. For a single detector, the rms variation in space-clamp levels ("clamp noise") is less than one count (out of 1024), and the variability in the space-clamp level among detectors is of the order of one count.

However, some relatively rare performance anomalies in the imagers have provided a reason to relativize. Before the spring of 1996, the visible imagery from both imagers experienced occasional incidents of severe striping, which consisted of positive or negative offsets, between 10 and 30 counts in magnitude, in the outputs of one of the eight detectors. The cause is believed to be noise spikes in the space clamps of the offending detector. Furthermore, for a few days around the equinoxes, the space clamp level of physical detector 6 of the GOES-9 imager's visible-channel array was observed to increase by approximately five counts for a few hours of the day, which also caused image striping. Relativization should prevent such anomalies from causing stripes in the images. Relativization would also be of benefit for the sounders. Because they do not clamp on space, their outputs show diurnal and seasonal drifts and detector-to-detector variations, tens of counts (out of 8192) in magnitude.

Table 4. Dates relativization was first enabled

Instrument		Date
Space	Imager	5/23/96
	Sounder	6/19/96
Blackbody	Imager	4/16/96
	Sounder	4/16/96

Therefore, in the spring of 1996 (see Table 4), relativization of the visible-channel imagery from the imagers and sounders was made operational. The data are relativized before being normalized. Relativization requires two steps. First, the mean count value from the most recent space look is subtracted from the pixel counts. (For the imager, the space-look data are from the post-clamp following the preceding space look.) Second, a constant count level, X_0, is added back in. Without the second step, relativization would have two undesirable consequences. First, when space itself is the target, the distribution of the data would be approximately Gaussian with a mean of zero. Half of the distribution would have count values less than zero and would be lost, since GVAR (the GOES VARiable format data stream, which users receive) will not accommodate negative integers. Second, the overall brightness of the image would change significantly between the "relativization off" and "relativization on" states.

For all eight visible-channel detectors of all imagers, the value of X_0 is 29. For all four visible-channel detectors of all sounders, the value of X_0 is 920. Since these are the nominal values for the space-count levels in the absence of relativization, there is hardly any change in overall image brightness between the "relativization off" and "relativization on" states.

At first glance, it may seem that the two steps of relativization would cancel each other out. This is not the case, however, because the mean space value and X_0 are not necessarily equal. The mean space-count level varies from space look to space look, as it is affected by noise (imager) or noise and drift (sounder), whereas X_0 is invariant.

6.3 Calibration

Although the visible detector-channels are not calibrated in orbit, calibration coefficients measured by ITT before launch[6] are transmitted to users in the GVAR data stream. A factor that converts radiance to reflectance factor, or effective albedo, is included as well. Since detector responsivities can vary unpredictably, the pre-launch calibration may not be valid after launch.

The calibration equation is either

Equation 10

$$R = mX + b$$

or

Equation 11

$$R = m(X - X_{sp}),$$

where X is the instrument output in counts, the subscript sp refers to the view of space, and m and b are the calibration coefficients measured before launch[6]. For each visible-channel detector, the radiance R is the average of the spectral (monochromatic) radiance over the spectral response function for that detector, i.e.,

$$R = \frac{\int R(\lambda)\,\Phi(\lambda)\,d\lambda}{\int \Phi(\lambda)\,d\lambda},$$

where l is wavelength in μm, F the spectral response function, and R(l) the spectral radiance of the target. Units of R are W/(m^2-sr-μm).

The value of b in Eq. (10) depends on the electronic zero level. As was discussed in the preceding section, this level varies with a standard deviation of approximately one count for the imagers and tens of counts for the sounder. Therefore, when the satellite is in orbit, the value of b determined in the laboratory (or at any other earlier time) may not be valid. Equation (11) is preferred.

Furthermore, relativization and normalization affect the calibration. Currently, visible-channel data from the imagers, but not the sounders, are being normalized. Since normalization makes the responses from all eight imager detectors the same as that of the reference detector, users of the pre-launch calibration of the imagers should apply the calibration coefficients for the reference detector (identified in Table 5) to the data from all detectors.

With relativization enabled, an instrument's output at the view of space is modified slightly, and the value of b in the calibration equation (Eq. [10]) needs to be modified accordingly. For this reason also, the best approach is to use Eq. (11). If Eq. (10) must be used, then the value of b should be determined from the equation: $b = -mM_0$

$$b = -mX_0,$$

in which, for the imagers, m is the slope for the reference detector. For the sounders, it is the slope for an individual detector. Values of b determined in this way, as well as the values of m (from Ref. 6) and X_0, appear in Tables 5 and 6.

The reflectance factor (or effective albedo) is obtained[6] from the radiance by

$$A = \kappa R,$$

where

$$\kappa = \pi/H,$$

and where H is the solar spectral irradiance H(l) averaged over the spectral response function of the visible detector, i.e.,

$$H = \frac{\int H(\lambda)\,\Phi(\lambda)\,d\lambda}{\int \Phi(\lambda)\,d\lambda}.$$

Values of H were computed[6] by ITT from tables of solar irradiance vs wavelength provided by Rossow et al.[13], whose values are based on measurements by Neckel and Labs[14]. The values of A lie between 0 and 1. When A has the value of 1, it corresponds to the radiance of a perfectly reflecting diffuse surface illuminated at normal incidence when the sun is at its annual-average distance from the Earth. Values of k appear in Tables 5 and 6.

Table 5. Visible-channel calibration coefficients for imagers

Satellite	GOES-8	GOES-9
Identity of reference detector (number in physical array)	2	3
m (reference detector) (W/(m^2-sr-m-count))	0.5501873	0.5492361
X_0	29	29
b (W/(m^2-sr-μm))	-15.955	-15.928
k ((m^2-sr-μm)/W)	1.92979 x 10^{-3}	1.94180 x 10^{-3}

Table 6. Visible-channel calibration coefficients for sounders

Satellite	Detector No.	m (W/(m^2-sr-μm-count))	X_0	b (W/(m^2-sr-μm))	k ((m^2-sr-μm)/W)
GOES-8	1	6.482527 x 10^{-2}	920	-59.64	2.2008 x 10^{-3}
	2	6.522216 x 10^{-2}		-60.00	
	3	6.560241 x 10^{-2}		-60.35	
	4	6.642020 x 10^{-2}		-61.11	
GOES-9	1	6.416324 x 10^{-2}	920	-59.03	2.2919 x 10^{-3}
	2	6.427129 x 10^{-2}		-59.13	
	3	6.523361 x 10^{-2}		-60.01	
	4	6.489786 x 10^{-2}		-59.71	

7. RETRANSMITTED (GVAR) DATA

Raw imager and sounder data are transmitted to the Command and Data Acquisition Station (CDA) at Wallops, VA, continuously in real time. Raw imager data are in 10-bit words, raw sounder data in 13-bit words. This section describes the subsequent data flow at the CDA culminating in the retransmission of processed data to users in the GVAR data stream.

7.1 Infrared-channel data

Calibration processing for the infrared channels takes place at the CDA in real time. In the processing, the calibration coefficients are computed and are applied to the raw data, converting them to radiances, as previously discussed. The radiances are scaled linearly so that they utilize the full 10-bit (imager) or 16-bit

(sounder) word length of the GVAR. The calibration coefficients (three per channel/detector) and the scaling coefficients (two per channel) are also transmitted in the GVAR. Users can derive the radiances from GVAR counts by inverting the scaling operation. The procedure for converting GVAR counts to radiances, temperatures, and eight-bit "mode-A" counts[15] is described in detail in Appendix A. For the sounders, the GVAR will contain both radiances and raw data. For the imagers, it will only contain the radiances, because the GVAR does not have enough bandwidth for both. The GVAR also contains statistical data and telemetry information for monitoring the calibration and instrument.

7.2 Visible-channel data

The raw data in the visible channels are relativized and normalized at the CDA, but no calibration is applied. The GVAR stream contains the imager data in 10-bit words and the sounder data in 16-bit words. The imager data are currently relativized and normalized, the sounder data relativized only. The GVAR also carries on/off flags for the status of relativization and normalization, as well as the values of X_0 (the constant space output) , the normalization look-up tables, the identity of the reference detector, and an identifier (including the creation date) of the normalization look-up tables. In addition, it contains the visible-channel pre-launch calibration coefficients (three per detector, but with the quadratic coefficients identically zero) and the factor that converts radiance to reflectance factor.

8. CONCLUSION

This memorandum describes the calibration processing in the GOES I-M ground system as of the summer of 1996. Two years earlier, when the GOES-8 satellite was launched, the processing utilized a simpler algorithm. Contingency paths were available in the software to deal with likely data irregularities, but they were not being used. Now, the processing has been changed to overcome the effects of instrument problems, some anticipated and some not, that were revealed in orbit. As continued monitoring of the data exposes more subtle performance anomalies, and as aging hardware presents new problems, the processing will probably continue to evolve.

ACKNOWLEDGEMENTS

The authors thank Roy Galvin of ITT and Edward Wack of MIT/Lincoln Laboratory for assistance with analyses of pre-launch test data; Brent Goddard of NOAA/NESDIS for assistance during check out and routine operations; Tim Schmit of the University of Wisconsin for computing the GVAR scaling coefficients; Donald Mack of Integral Systems, Inc., Marvin Maxwell and William Bryant, Jr. of Swales and Associates, Inc., and Opal Chen and John Gaiser of Space Systems/Loral for valuable advice; W. P. Menzel and C. R. N. Rao of NOAA/NESDIS for critical readings of the manuscript.

APPENDIX A: INTERPRETATION OF INFRARED DATA IN GVAR

In the GVAR data stream, the data from the infrared channels of the imagers and sounders are scaled radiances packaged in 10-bit and 16-bit words, respectively. The conversion of the raw data from the instruments to scaled radiances is carried out in real time in the Sensor Processing System computers at the Command and Data Acquisition facility at Wallops, VA, and is described in the body of this paper. This appendix describes how users may convert the ten-bit GVAR count values (0-1023) in channels 2 - 5 of the imagers and the 16-bit GVAR count values (0-65535) in channels 1-18 of the sounders back to scene radiances, brightness temperatures, and eight-bit mode-A counts[15].

The first step is to convert GVAR counts to radiances with the following equation:

$$\mathbf{R = (X_G - B)/ M ,}$$

where R is radiance in mW/(m^2-sr-cm-1) and X_G is the GVAR count value. The coefficients M and B are the "scaling" slope and intercept, respectively, and appear in Tables A1 and A2. The units of M are counts/(mW/[m^2-sr-cm^{-1}]). Their values depend only on channel, not detector, and for a given channel we expect them to be constant for all time and to be the same for each satellite of the series.

Table A1. GOES imagers scaling coefficients

Channel	M	B
2	227.3889	68.2167
3	38.8383	29.1287
4	5.2285	15.6854
5	5.0273	15.3332

Table A2. GOES sounders scaling coefficients

Channel	M	B

1	528.9773	1745.625
2	540.0049	1566.014
3	485.6243	1311.186
4	394.5752	887.7943
5	357.8019	787.1643
6	334.1747	417.7184
7	311.5226	249.2180
8	314.6032	251.6826
9	434.3518	716.6805
10	1126.224	900.9795
11	1899.565	1139.739
12	2874.342	2155.757
13	9642.747	626.7785
14	14105.38	916.8496
15	26221.34	1704.387
16	10720.60	428.8239

17	12136.11	497.5806
18	19358.13	348.4463

To convert radiance to temperature, one first uses the following formula (the inverse of the Planck function) to derive "effective" temperature:

$$\mathbf{T_{eff} = (c_2 n)/\ln(1 + [c_1 n^3]/R)} \ ,$$

where T_{eff} is effective temperature (K), "ln" stands for natural logarithm, and R is radiance. The coefficients c1 and c2 are the two radiation constants, given by

$c_1 = 1.191066\text{x}10\text{-}5$ mW/(m^2-sr-cm^{-4})

$c_2 = 1.438833$ K/cm^{-1}

The quantity n is the central wavenumber of the channel. For a given channel it may vary slightly among detectors, and it will vary from instrument to instrument. The values of appear in tables A3-A6.

To convert effective temperature T_{eff} to actual temperature T (K), one uses the following formula:

$$\mathbf{T = bT_{eff} + a},$$

The constants **n**, **a**, and **b** and depend on channel, detector, and instrument and appear in Tables A3-A6.

The use of T_{eff} accounts for the variation of the Planck function across the spectral passband of the channel. The differences between the values of T and T_{eff} increase with decreasing temperature. They are usually of the order of 0.1K. In the worst case, near 180K, they are approximately 0.3K.

The mode - A count value X_a is derived from the temperature with the following equations[15]:

$$\mathbf{For\ 163K <= T <= 242K, \quad X_a = 418 - T.}$$

$$\mathbf{For\ 242K <= T <= 330K, \quad X_a = 660 - 2T.}$$

Mode-A count values are on an eight-bit scale and range in value from 0 to 255, with high counts representative of low temperatures. Beyond the difference in precision, there is a fundamental difference between GVAR counts and mode-A counts--their units. GVAR counts are scaled radiances, whereas mode-A counts are temperatures.

Tables of GVAR counts, radiances, temperatures, and mode-A counts will be provided by the first author on request.

Table A3. Constants for GOES-8 imager

Channel	Detector	n(cm^{-1})	a(K)	b
2	1	2556.71	-0.578526	1.001512
2	2	2558.62	-0.581853	1.001532
3	1	1481.91	-0.593903	1.001418
4	1	934.30	-0.322585	1.001271
4	2	935.38	-0.351889	1.001293
5	1	837.06	-0.422571	1.001170
5	2	837.00	-0.466954	1.001257

Table A4. Constants for GOES-9 imager

Channel	Detector	n(cm^{-1})	a(K)	b
2	1	2555.18	-0.579908	1.000942
2	2	2555.18	-0.579908	1.000942
3	1	1481.82	-0.493016	1.001076
4	1	934.59	-0.384798	1.001293
4	2	934.28	-0.363703	1.001272
5	1	834.02	-0.302995	1.000941
5	2	834.09	-0.306838	1.000948

Table A5. Constants for GOES-8 sounder

Channel	Detector	n(cm^{-1})	a(K)	b

1	1	680.59705	0.0011541479	1.0000183
1	2	680.51139	0.0047380732	1.0000086
1	3	680.81462	0.0014610959	1.000018
1	4	680.73182	-0.00042293612	1.0000216
2	1	695.92447	-0.067530673	1.0001987
2	2	695.93168	-0.069026616	1.0002026
2	3	696.1214	-0.073060464	1.0002117
2	4	695.8373	-0.056595405	1.0001696
3	1	711.80216	-0.010171243	1.0000582
3	2	711.8637	-0.015032924	1.0000701
3	3	711.96416	-0.011705031	1.0000615
3	4	711.80891	-0.011002261	1.0000614
4	1	732.48438	-0.0042959367	1.0000392
4	2	732.39916	-0.0040822167	1.0000379
4	3	732.46298	-0.0051373478	1.0000106
4	4	732.46931	-0.0049827181	1.0000101
5	1	747.75312	-0.037536733	1.0001166
5	2	747.53399	-0.031523095	1.0001032
5	3	747.59143	-0.031117282	1.0001025
5	4	747.48321	-0.022986702	1.0000855
6	1	790.5998	-0.09722985	1.0002888
6	2	790.39692	-0.093920988	1.0002841

6	3	790.35717	-0.089752097	1.0002749
6	4	791.35802	-0.13292141	1.0003539
7	1	827.63841	-0.0232754	1.0003278
7	2	830.40346	-0.19918135	1.0006315
7	3	829.32451	-0.13434617	1.0005204
7	4	827.61148	0.017236714	1.0002605
8	1	906.81053	-0.15212177	1.0004685
8	2	906.20913	-0.15912377	1.0004923
8	3	906.91478	-0.18977748	1.0005115
8	4	907.56109	-0.2034948	1.0005222
9	1	1029.7209	-0.045072033	1.0001371
9	2	1029.6963	-0.043802031	1.000135
9	3	1029.2687	-0.033910527	1.0001365
9	4	1029.3769	-0.035802096	1.0001361
10	1	1339.7687	-0.15379456	1.0003742
10	2	1339.2473	-0.14469896	1.0003929
10	3	1339.5185	-0.14680066	1.0003878
10	4	1339.5473	-0.14827852	1.0003824
11	1	1421.09	-0.23363311	1.0007483
11	2	1421.8586	-0.24877913	1.0006982
11	3	1420.6829	-0.21459881	1.0007938
11	4	1422.4471	-0.26186387	1.0006938

12	1	1536.2837	-0.16825513	1.000216
12	2	1535.3069	-014374678	1.0002864
12	3	1537.5272	-0.23662459	1.0000769
12	4	1535.0548	-0.16469406	1.0002578
13	1	2184.7961	-0.01849728	1.0000665
13	2	2184.7961	-0.01849728	1.0000665
13	3	2184.7961	-0.01849728	1.0000665
13	4	2184.7961	-0.01849728	1.0000665
14	1	2207.5585	-0.023929612	1.0000191
14	2	2207.5585	-0.023929612	1.0000191
14	3	2207.5585	-0.023929612	1.0000191
14	4	2207.5585	-0.023929612	1.0000191
15	1	2247.5698	-0.034093166	0.99993075
15	2	2247.5698	-0.034093166	0.99993075
15	3	2247.5698	-0.034093166	0.99993075
15	4	2247.5698	-0.034093166	0.99993075
16	1	2422.0784	-0.066306989	1.000011
16	2	2422.0784	-0.066306989	1.000011
16	3	2422.0784	-0.066306989	1.000011
16	4	2422.0784	-0.066306989	1.000011
17	1	2509.4001	-0.060780208	1.0001174
17	2	2509.4001	-0.060780208	1.0001174

17	3	2509.4001	-0.060780208	1.0001174
17	4	2509.4001	-0.060780208	1.0001174
18	1	2664.7035	-0.34148389	1.0009243
18	2	2664.7035	-0.34148389	1.0009243
18	3	2664.7035	-0.34148389	1.0009243
18	4	2664.7035	-0.34148389	1.0009243

Table A6. Constants for GOES-9 sounder

Channel	Detector	n(cm^{-1})	a(K)	b
1	1	681.53264	-0.061569679	1.0001824
1	2	681.40135	-0.053410761	1.0001603
1	3	681.52794	-0.090823775	1.0002626
1	4	681.23907	-0.049632175	1.0001508
2	1	694.26673	-0.035721417	1.0001135
2	2	694.09261	-0.026237608	1.0000894
2	3	693.93184	-0.014017787	1.0000574
2	4	694.11597	-0.026341654	1.0000893
3	1	711.39629	-0.043973934	1.0001314
3	2	711.25223	-0.035778771	1.0001112
3	3	711.00519	-0.026554312	1.0000877
3	4	711.07759	-0.025028536	1.0000841
4	1	732.56429	-0.031778653	1.0000973

4	2	732.50229	-0.028546325	1.0000897
4	3	732.50527	-0.032654323	1.0000997
4	4	732.33055	-0.025780988	1.0000829
5	1	747.19713	-0.043470631	1.0001236
5	2	747.1825	-0.04211854	1.0001205
5	3	746.83467	-0.020193021	1.0000714
5	4	746.91053	-0.03125795	1.0000972
6	1	789.55684	-0.065385221	1.0002199
6	2	789.72841	-0.072530803	1.0002344
6	3	789.84766	-0.080716615	1.0002493
6	4	789.35098	-0.056105065	1.0001998
7	1	826.87703	0.041396369	1.000228
7	2	827.22901	0.0274577	1.0002501
7	3	828.27187	-0.087133142	1.000445
7	4	828.67767	-0.069590619	1.0004218
8	1	911.22294	-0.30550413	1.0006317
8	2	910.73052	-0.28258246	1.0006113
8	3	909.80214	-0.23979418	1.0005719
8	4	909.70281	-0.22061492	1.0005457
9	1	1028.9077	-0.058287786	1.0001362
9	2	1028.8798	-0.054285716	1.0001341
9	3	1028.7845	-0.055189391	1.000134

9	4	1028.8579	-0.055101679	1.0001342
10	1	1335.2658	-0.1131839	1.0004206
10	2	1335.8313	-0.13015363	1.0003907
10	3	1336.0503	-0.13414168	1.0003834
10	4	1335.8627	-0.1304702	1.0003901
11	1	1420.8469	-0.2383551	1.0007496
11	2	1421.0338	-0.24007956	1.0007414
11	3	1420.6599	-0.23051649	1.0007729
11	4	1420.7697	-0.23480823	1.000752
12	1	1529.1783	-0.18721929	1.000148
12	2	1529.4056	-0.19578939	1.0001144
12	3	1529.2363	-0.17817533	1.0001506
12	4	1529.6935	-0.20017465	1.0001009
13	1	2183.9199	-0.019638376	1.0000246
13	2	2183.9199	-0.019638376	1.0000246
13	3	2183.9199	-0.019638376	1.0000246
13	4	2183.9199	-0.019638376	1.0000246
14	1	2207.0082	-0.024176572	0.99999895
14	2	2207.0082	-0.024176572	0.99999895
14	3	2207.0082	-0.024176572	0.99999895
14	4	2207.0082	-0.024176572	0.99999895
15	1	2245.837	-0.029091526	0.99994699

15	2	2245.837	-0.029091526	0.99994699
15	3	2245.837	-0.029091526	0.99994699
15	4	2245.837	-0.029091526	0.99994699
16	1	2415.1642	-0.051874656	1.000095
16	2	2415.1642	-0.051874656	1.000095
16	3	2415.1642	-0.051874656	1.000095
16	4	2415.1642	-0.051874656	1.000095
17	1	2512.0862	-0.063295056	1.0000751
17	2	2512.0862	-0.063295056	1.0000751
17	3	2512.0862	-0.063295056	1.0000751
17	4	2512.0862	-0.063295056	1.0000751
18	1	2665.3491	-0.28151318	1.0007142
18	2	2665.3491	-0.28151318	1.0007142
18	3	2665.3491	-0.28151318	1.0007142
18	4	2665.3491	-0.28151318	1.0007142

REFERENCES

1. Bradley, C. (ed.), "The GOES I-M system functional description," NOAA Technical Report NESDIS 40, U.S. Dep't. Commerce, National Oceanic and Atmospheric Administration, Washington, D.C., 126 pp. (1988).
2. Space Systems/Loral, *GOES I-M Data Book*, prepared for NASA/GSFC under contract NAS5-29500, 184 pp. (1994).
3. Menzel, W.P. and J. F.W. Purdom, "Introducing GOES-I: The first of a new generation of geostationary operational environmental satellites," *Bull. Amer. Meteorol. Soc.*, **75**, 757-781 (1994).
4. Menzel, W.P., W.L. Smith, and L.D. Herman, "Visible infrared spin-scan radiometer atmospheric sounder radiometric calibration: an in-flight evaluation from intercomparisons with HIRS and radiosonde measurements," *Appl. Opt.*, **20**, 3641-3644 (1981).
5. Bremer, J.C. and G.J. Comeyne, "Optimization of the GOES-I imager's radiometric accuracy: drift and 1/f noise suppression," *Optical Engineering*, **33**, 3324 (1994).
6. (a) ITT Aerospace/Communications Div. (Ft. Wayne, IN), "GOES-IJ/KLM SN03 Imager data and calibration handbook," submitted by Space Systems/Loral, Palo Alto, CA, and prepared for NASA, Greenbelt, MD, 15 Jan. 1994.

   (b) ITT Aerospace/Communications Div. (Ft. Wayne, IN), "GOES-IJ/KLM SN03 Sounder data and calibration handbook," submitted by Space Systems/Loral, Palo Alto, CA, and prepared for NASA, Greenbelt, MD, 15 Jan. 1994.

   (c) ITT Aerospace/Communications Div. (Ft. Wayne, IN), "GOES calibration and alignment handbook for the Imager SN04 instrument," submitted by Space Systems/Loral, Palo Alto, CA, and prepared for NASA, Greenbelt, MD, Sept. 1994.

   (d) ITT Aerospace/Communications Div. (Ft. Wayne, IN), "GOES SN04 Sounder calibration and alignment handbook," submitted by Space Systems/Loral, Palo Alto, CA, and prepared for NASA, Greenbelt, MD, Dec. 1994.
7. (a) Cousins, D., E.C. Wack, and R.M. Heinrichs, "GOES SN03 Imager final thermal vacuum IR calibration results," MIT/Lincoln Laboratory proj. rept. NOAA-5, prepared for the National Oceanic and Atmospheric Administration under Air Force contract F19628-90-C-0002, 163 pp., Sept. 1, 1993.

   (b) Heinrichs, R.M., D. Cousins, and E.C. Wack, "GOES SN03 Sounder final thermal vacuum

IR calibration results," MIT/Lincoln Laboratory proj. rept. NOAA-8, prepared for the National Oceanic and Atmospheric Administration under Air Force contract F19628-90-C-0002, 156 pp., Nov. 9, 1993.

(c) Cousins, D., R.M. Heinrichs, and E.C. Wack, SN04 Imager IR calibration," MIT/Lincoln Laboratory proj. rept. NOAA-11, prepared for the National Oceanic and Atmospheric Administration under Air Force contract F19628-90-C-0002, 115 pp., Aug. 17, 1994.

(d) Wack, E.C., "SN04 Sounder IR calibration report," MIT/Lincoln Laboratory proj. rept. NOAA-14, prepared for the National Oceanic and Atmospheric Administration under Air Force contract F19628-95-C-0002, 137 pp., Mar. 14, 1995.

8. Weinreb, M.P., J.X. Johnson, J.C. Bremer, E.C. Wack, and O. Chen, "Algorithm to compensate for variation of reflectance of GOES-8 and -9 scan mirrors with scan angle," preprint volume, *8th Conf. on Satellite Meteorol. and Oceanography*, Atlanta, GA, (Amer. Meteorol. Soc., Boston, MA), pp. 110-114, Jan. 28-Feb. 2, 1996.
9. Nicodemus, F.E., "Directional reflectance and emissivity of an opaque surface," *Appl. Opt.*, **4**, 767 (1965).
10. Cafferty, M., "Reflectance measurements of the SN03 scan mirror witness sample," MIT/Lincoln Laboratory internal memo, 8 pp., 15 Aug. 1994.
11. Baucom, J. and M. Weinreb, "Characteristics of E/W stripes in infrared images from the GOES-8 Imager," in *GOES-8 and Beyond*, Edward R. Washwell, editor, Proc. SPIE 2812, 587-595 (1966).
12. Weinreb, M.P., J.X. Johnson (nee R. Xie), J.H. Lienesch, and D.S Crosby, "Destriping GOES images by matching empirical distribution functions," *Remote Sens. Environ.*, **29**, 185 (1989).
13. Rossow, W.R., E. Kinsella, A. Wolf, and L. Gardner, "Description of reduced radiance data," *International Satellite Cloud Climatology Project (ISCCP)*, WMO/TD-No. 58 (1985).
14. Neckel, H. and D. Labs, "The solar radiation between 3300 and 12500 A," *Solar Physics*, **90**, 205 (1984).
15. Bristor, C.L. (ed.), "Central processing and analysis of geostationary satellite data," NOAA Tech. Memo. NESS 64, U.S. Dep't. Commerce, National Oceanic and Atmospheric Administration, Washington, DC, 155 pp. (1975).